NASA TT F-11,473

SUPERSONIC FLOWS AROUND CONES AT INCIDENCE

René Gonidou

Translation of "Ecoulements Supersoniques Autour
de Cones en Incidence"
Office National d'Etudes et de Recherches Aérospatiales,
T.P. No. 523, Sept. 1967, 9 p.
La Recherche Aerospatiale, No. 120,
Sep.-Oct. 1967, pp 11-19.

NATIONAL AERONAUTICS AND SPACE ADMINISTRATION
WASHINGTON, D.C., 20546 JANUARY 1968

NOTATION

(z, r, φ)	System of cylindrical coordinates associated with the axis of the cone.
(u, v, w)	Axial, radial, circumferential components of the velocity corresponding to C_{cr}.
C_{cr}	Critical velocity of sound.
p	Pressure divided by the product of the upstream density and C_{cr}^2.
α, β	Parameters encountered in the notation for finite differences of $\frac{\partial X}{\partial \xi}$, $\frac{\partial X}{\partial \varphi}$.
σ	Coefficient of the viscosity term in $\frac{\partial^2 X}{\partial \varphi^2}$.
X	Vector of the components (u, v, w, p).
$\mathcal{A}, \mathcal{B}, \mathcal{C}$	Square matrices of order 4 dependent on X.
Γ	Vector with 4 components dependent on X.
$r = G(z, \varphi)$	Equation of the obstacle.
$r = F(z, \varphi)$	Equation of the shock.
$\xi = \frac{r - G}{F - G}$	Auxiliary variable used to facilitate the notation of the conditions at the limits
p_c	Pressure behind the shock.
p_∞	Pressure in the upstream flow (0.0793 for the example studied).
$I = 1 - \frac{p_\infty}{p_c}$	Parameter defining the intensity of the shock.
i	Angle of incidence of the wind.
β_k	Angle of half-aperture of the circular cone.
M_∞	Mach number upstream.

i_c	Angle of incidence for which the intensity of the shock becomes zero at $\varphi = \pi$.
λ	Ratio b/a of the axes for the cone with an elliptical section.
μ	Angle of deflection (half-aperture angle of the circular cone tangent at $\varphi = \pi/2$).

SUPERSONIC FLOWS AROUND CONES AT INCIDENCE

René Gonidou*

ABSTRACT. The paper presents some numerical results obtained at Mach 7 for the supersonic flow of a perfect gas around conical bodies (of circular or elliptical cross sections) at incidence.

The method of calculation employed is a direct method termed the method of "establishment" of the solution due to Babenko, Voskresenskiy, Lyubimov and Rusanov.

This study shows that the shock wave remains closed for angles of incidence greater than the half-aperture angle of the circular cone.

Starting with a certain incidence, the singular point of entropy located on the upper surface moves from the surface of the body toward the interior of the flow. Numerical instabilities then appear which make it impossible to continue the study up to higher angles of incidence where the shock becomes evanescent.

Introduction

/12**

The numerical determination of the flow of a perfect gas around cones (circular or not has been the subject of many studies in the last few years.

Various reverse or direct methods have been used to this end: among the latter, the method of "establishment" of Babenko, Voskresenskiy, Lyubimov and Rusanov (ref. 1; we shall designate it more conveniently by the BVLR method) seems to be of particular interest; it has made it possible to obtain tables of supersonic flows around circular cones at incidence which complete the Kopal tables.

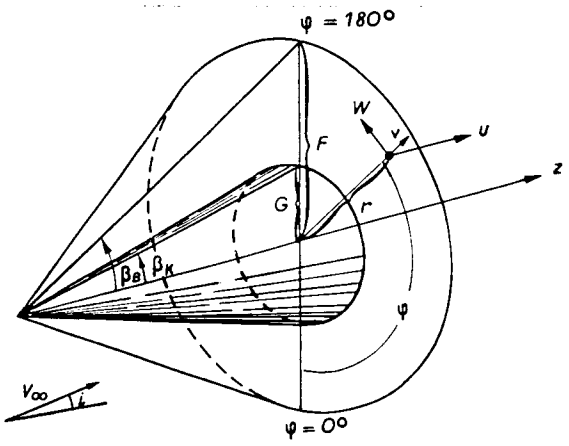

Figure 1. Coordinate System.

*The author expresses his sincere appreciation to Jean-Piere Guiraud, under whose direction this work was carried out.

**Numbers in the margin indicate pagination in the foreign text.

We chose this method to calculate the supersonic flow (Mach 7) around circular cones at incidences close to the half-aperture angle of the cone and around cones of elliptical section at similar incidence.

The analysis of the BVLR method and the detailed elaboration of the program were carried out with the very efficient assistance of the SEMA (Société d'Économie et de Mathématique Appliquées [Economics and Applied Mathematics Society], Paris). The calculations were performed on electronic equipment of the SIA (Société d'Informatique Appliquée [Applied Information Science Society]).

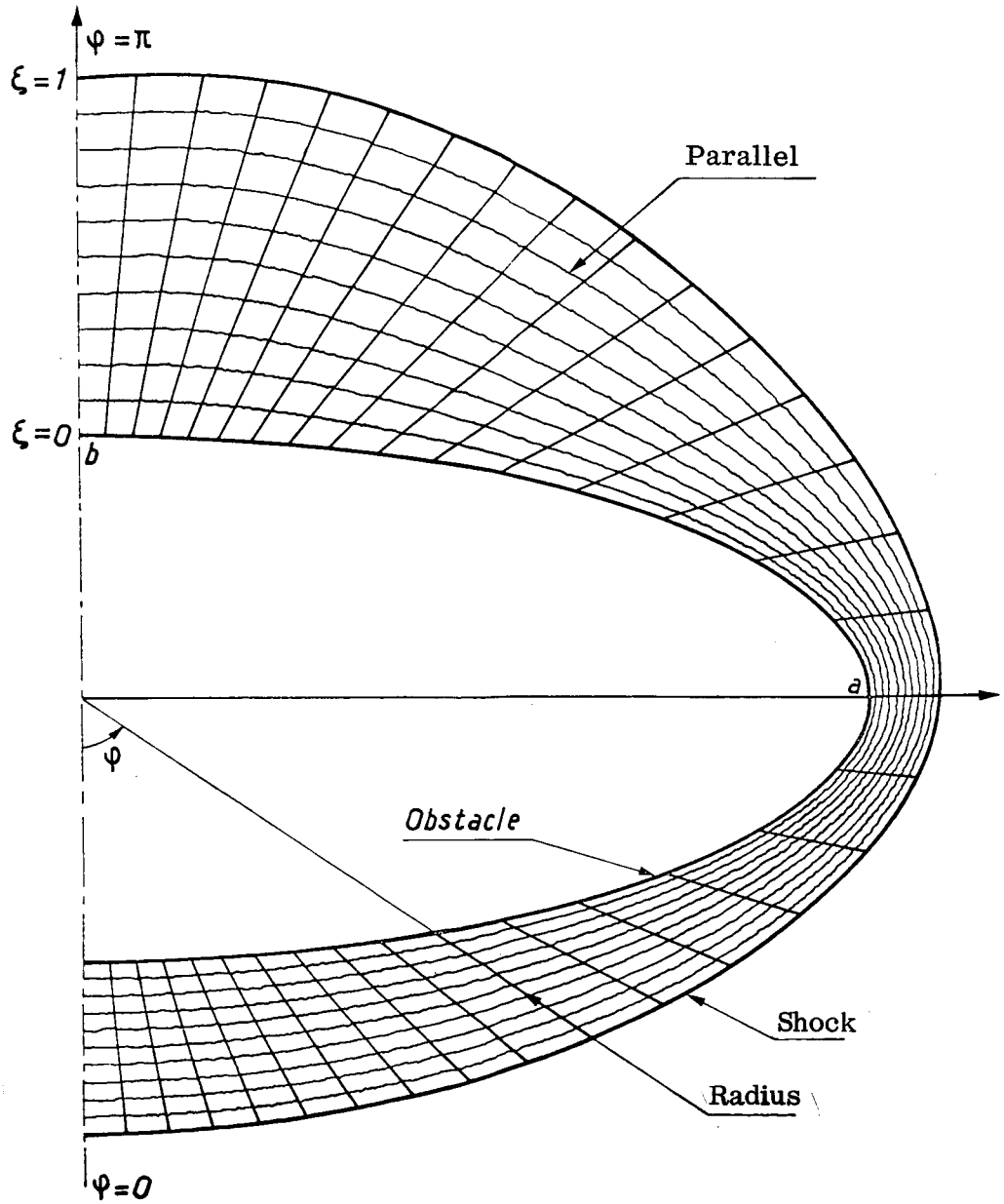

Figure 2. Grid Used for the Finite Difference Scheme.

Formulation of the Problem

/13

The BVLR method [1] reduces the study of the supersonic flow around a conical obstacle to the solution of a quasi-linear system with partial derivatives

$$A\frac{\partial X}{\partial z} + B\frac{\partial X}{\partial \xi} + C\frac{\partial X}{\partial \varphi} + \Gamma = 0.$$

from certain initial conditions in a plane $z = z_0$, taking into account the conditions of the limits at the boundaries

$\xi = 0$ (tangential velocity at the obstacle),
$\xi = 1$ (Rankine-Hugoniot conditions on the shock),

and on the periodicity in φ of the solution being sought.

The algorithm of the proposed calculation makes it possible to determine the flow in a plane $z_1 = z_0 + \Delta z$ from a known flow in plane z_0 by a method of finite differences; we shall represent the grid in (ξ, φ) in a half-plane perpendicular to the axis of the cone.

The flow in plane z_1 is obtained in an iterative manner after the successive solution of independent systems on each ray φ = constant, by means of an appropriate discretization of the partial differential equations.

On each radius:

a) The direct progression brings the condition relative to the obstacle on the shock and thus completes the Rankine-Hugoniot conditions,

b) The solution of the linearized system on the shock provides the position of the latter and the downstream aerodynamic quantities,

c) The inverse progression makes use of the preceding information for completely determining the flow between the shock and the obstacle.

This algorithm of calculation makes it possible to obtain the supersonic flow around an obstacle of conical shape asymptotically. The solution is established in the course of the progression in z starting from any initial data in a plane of abscissa z_0. When z tends to infinity, the solution obtained converges toward the conical flow being sought.

This so-called "establishment" method has a precise physical meaning; indeed, it is known that at a great distance from the apex, the shape of the nose of an ogive practically no longer intervenes on the upstream flow.

The convergence of the solution obtained toward that of stationary flow around conical bodies is not demonstrated theoretically, but it is fully corroborated by the analysis of the results of numerous calculations.

Remarks:

1. BVLR introduce certain parameters into the difference equations for purposes of stability: σ carries a viscosity count, α and β balance the iterative scheme. The choice of: $\sigma = 10^{-4}$; $\alpha - \beta = 10^{-2}$ gives a reasonable truncation error in the different cases treated.

2. The stability of the method is related to conditions which bring in the field of the velocities and the grid with finite differences. The stability conditions are no longer verified at high incidences for a scheme utilizing a linear function ξ between the shock and the obstacle. These considerations have determined the scope of the use of the algorithm in our case.

3. The matrices $\mathcal{A}$, $\mathcal{B}$, $\mathcal{C}$ employed here are slightly different from those of BVLR [1]; indeed, we have reduced the dimensions of vector X to 4 components (u, v, w, p) by expressing the density as a function of the pressure and velocity.

Circular Cones at Incidence

The above-described BVLR method was programmed on a data processor, and a special study was made of supersonic flow at Mach 7 around a circular cone (C) of half-aperture $\beta_k = 9°$ at different incidences i ranging from 5 to 11°.

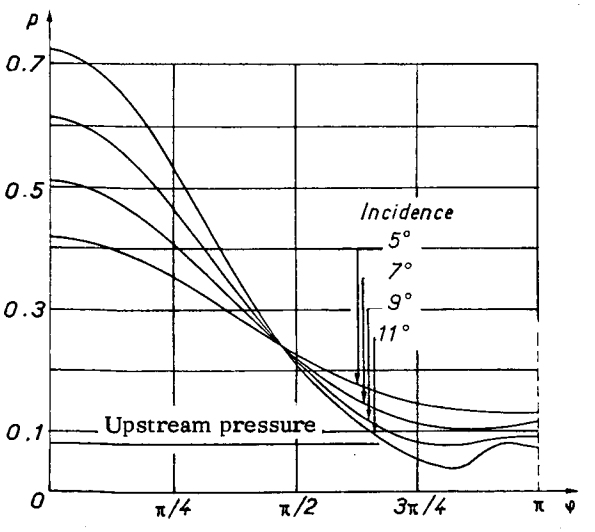

Figure 3. Pressure on the Circular Cone (C) at Incidence.

The initial data were given by flow around a circular cone with a half-aperture of 10° at a 5° incidence (BVLR tables [1]). We determined the flow around (C) at a 5° incidence, then increased the incidence (5, 7, 9, 10, 11°, respectively), each time taking the flow obtained in the preceding stage as the initial data.

The grid employed consisted of 16 "radii" on a half-circumference and 10 "parallels" (ξ = constant) between the shock and the obstacle (obviously, symmetry considerations on axes $\varphi = 0$ and $\varphi = \pi$ replaced the more general conditions of 2π - periodicity in φ of the solution).

We focused our attention on some specific types of behavior: pressure and circumferential component of the velocity on the body. We also give a more overall course of the flow with isopiestic curves and the field of entropic direction

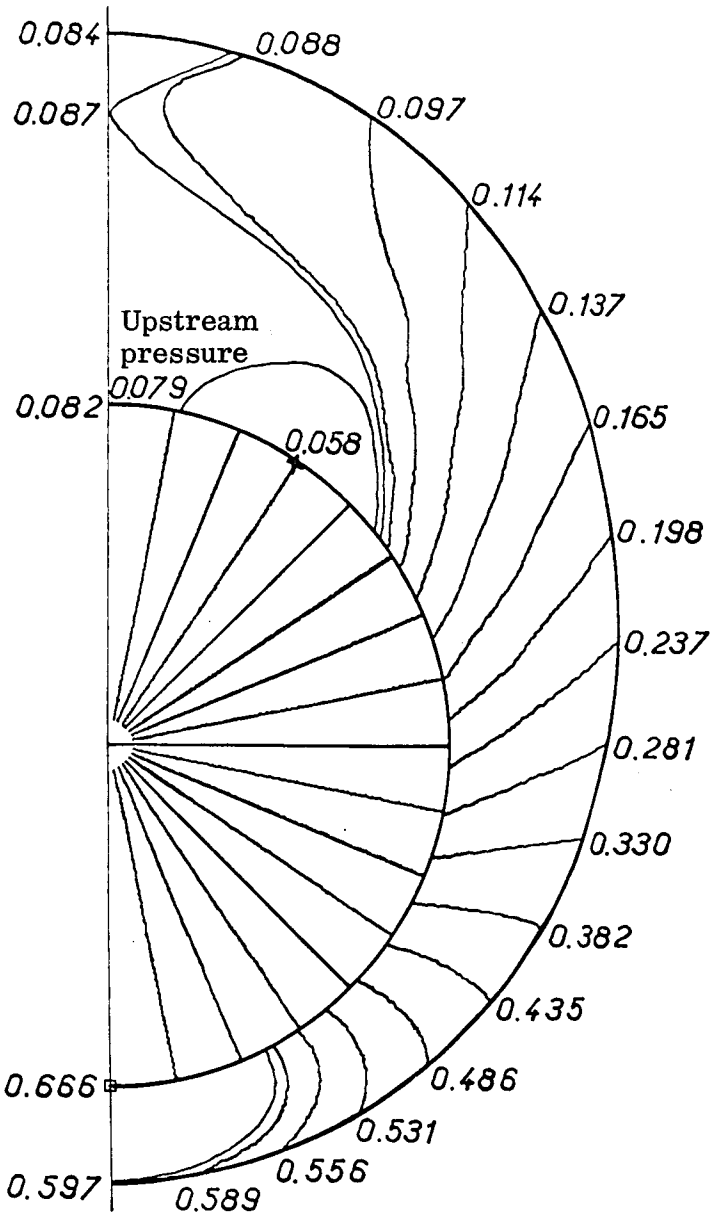

Figure 4. Curves p = Constant Around (C) at 10° Incidence.

(in a section by a half-plane perpendicular to the axis of the cone, at each point we draw a small segment whose direction gives the direction of the tangent to the isentrope).

1. Pressure on the Obstacle

Up to an incidence of 5°, the distribution of pressure on the obstacle as a function of angle φ is continuous, decreasing, and the curve has the shape of an arc of sinusoid. When the incidence increases, a pressure minimum appears on the "leeward" side, this minimum being very marked for an incidence of 11°. For incidences greater than the half-aperture angle of the cone, there exists a zone which is in a depression relative to the flow at infinity; the minimum amounts to 0.04, i.e., approximately one-half of the upstream pressure for i = 11°. /14

Let us also note that for an angle φ close to 85°, the pressure on the obstacle is practically independent of the incidence.

The pressure maximum is located on the axis of symmetry of the obstacle on the windward side; the minimum is also on the body, but at φ = 150°. A local maximum exists on the axis of symmetry inside the flow for φ = 180°.

2. Intensity of the Shock

We measured the intensity of the shock by the ratio $I = \frac{p_c - p_\infty}{p_c}$, representing the relative discontinuity of the pressures at each point of the grid located on the shock.

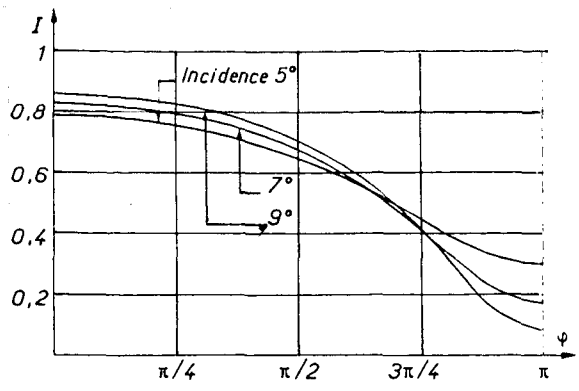

Figure 5. Intensity of the Shock for Different Incidences.

($\beta_K = 9°$, $M_\infty = 7$).

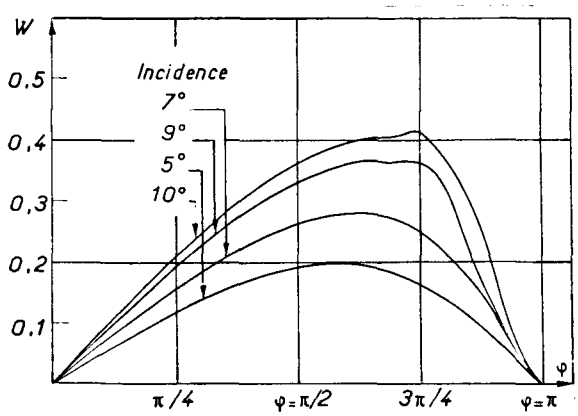

Figure 6. Component w on the Circular Cone (C).

($\beta_K = 9°$, $M_\infty = 7$).

The intensity of the shock on the windward side decreases rapidly when the incidence increases. A polynomial extrapolation from values of I (at $\varphi = \pi$) seems to indicate that the shock wave degenerates into a Mach wave on the axis of symmetry on the leeward side for an incidence close to $i_c = 12°$. At lower incidences, the shock wave remains closed all around the obstacle, and calculations carried out for 1 = 10° and 11° confirm this phenomenon.

3. Field of Velocities

The axial and radial components of the velocity vary regularly in the entire flow and on the body in particular. On the other hand, the circumferential component exhibits an essentially nonlinear behavior and, in particular, presents very substantial relative variations on the obstacle.

The function $w(\varphi)$ has a maximum on the leeward side; when the incidence increases, this maximum moves in the direction of increasing φ; for $i > 9°$, the slope becomes very pronounced, and the curve becomes less regular.

Figures 7 and 8 show that in the vicinity of the axis of symmetry of the leeward side, the shock is very close to the upstream Mach cone for flows with large incidences; the intensity of the shock is very week in this region. /15

In Figure 8 we note that the tangent to the isentrope passing through point M is directed toward the inside of the flow (above the line ξ = constant passing through this point). It therefore appears that the node S, a singular point of entropy, which at smaller incidences is at the intersection of H of the body and of the axis of symmetry (Fig. 7), has a tendency to move toward the interior of the flow when the incidence increases as indicated in Fig. 8. This clearly illustrates the fact that the entropy is constant on the obstacle, as was recognized long ago by Ferri [2].

These numerical results agree with a study of Melnik [3], which reports on the behavior of entropy singularities in the flow around a circular cone as a function of incidence.

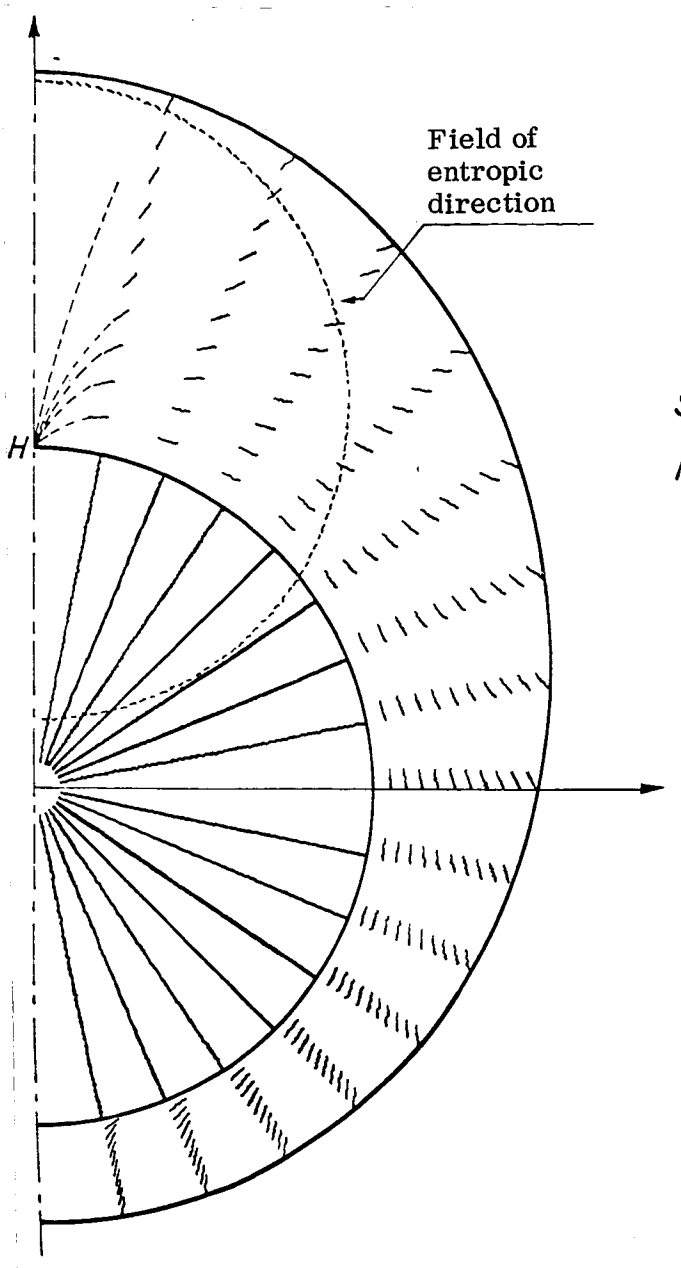

Figure 7. Field of Entropic Direction.
($\beta_K = 9°$, $M_\infty = 7$), $i = 10°$.

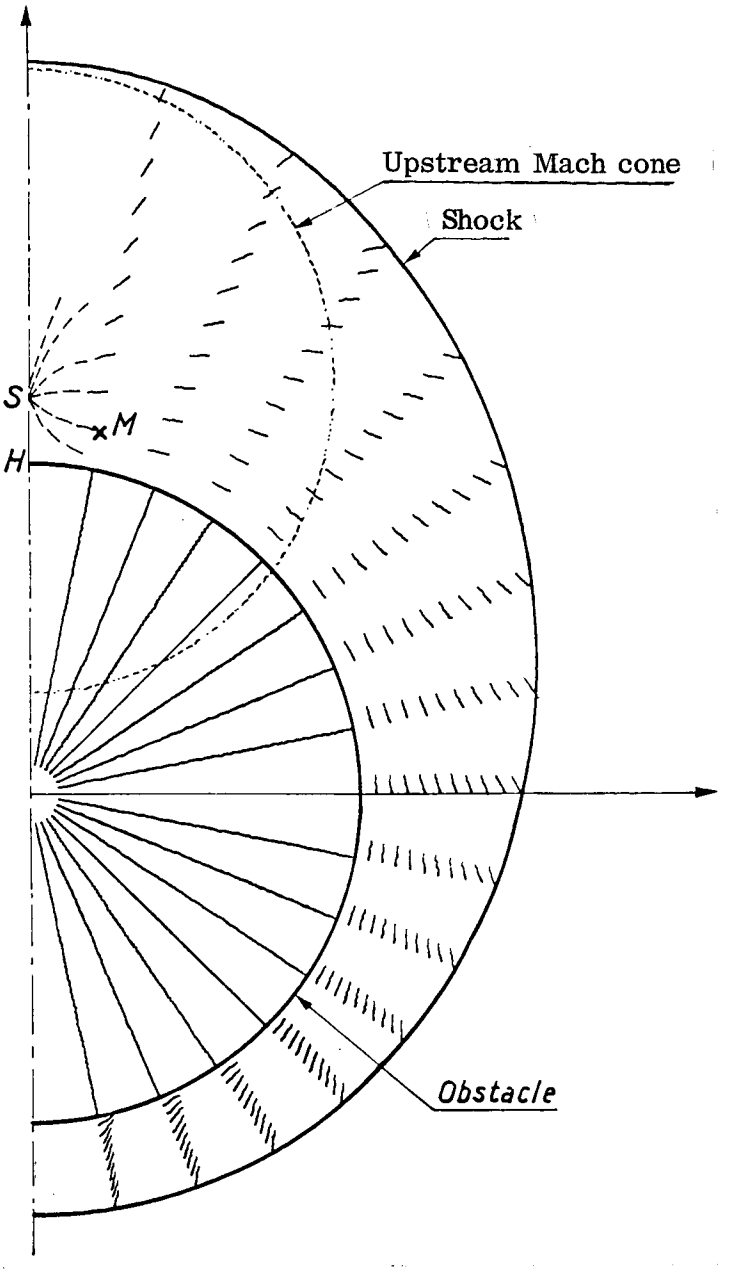

Figure 8. Field of Entropic Direction.
($\beta_K = 9°$, $M_\infty = 7$), $i = 11°$.

Unfortunately, the BVLR method employed here with the above-described grid becomes unstable as a result of these singularities and no more definite conclusions can be drawn regarding the preceding phenomenon.

This numerical instability also makes it impossible to continue the use of this method at higher incidences up to the appearance of an evanescent shock wave. /16

Elliptical Cones at Incidence

Using initial data corresponding to the flow around a circular cone of 20° half-aperture at a 5° incidence (BVLR Tables [1]), we established the flow at Mach 7 around different cones of elliptical section having a 20° angle of deflection μ and whose ratio of axes varies from 1 to 113.

The flow around an elliptical cone E_2 of ratio $b/a = \lambda_2$ is obtained at the limit, for z tending to infinity, of flow around an ogive whose node is constituted by an elliptical cone $E_1(\lambda_1)$ ending in cone E_2. The final cone E_2 and frontal cone E_1 are joined by an intermediate portion with a continuous curvature (here a polynomial function of z of degree 5 on each radius). We studied elliptical cones characterized by $\lambda_i = 0.8$, 0.64, 0.5, 0.4 and 1/3, respectively, retaining the same deflection (i.e., with the starting circular cone as the tangent cone).

When the ratio λ becomes less than 0.5, the curvature varies rapidly in the vicinity of the major axis and it is important to use a sufficiently fine grid (32 radii on a half circumference) in order to give a true representation of variations of the aerodynamic quantities.

Cone (E) of elliptical section of ratio $b/a = 1/3$ was studied at different incidences $i = 5$, 7, and 9° in a manner analogous to that of the circular cone.

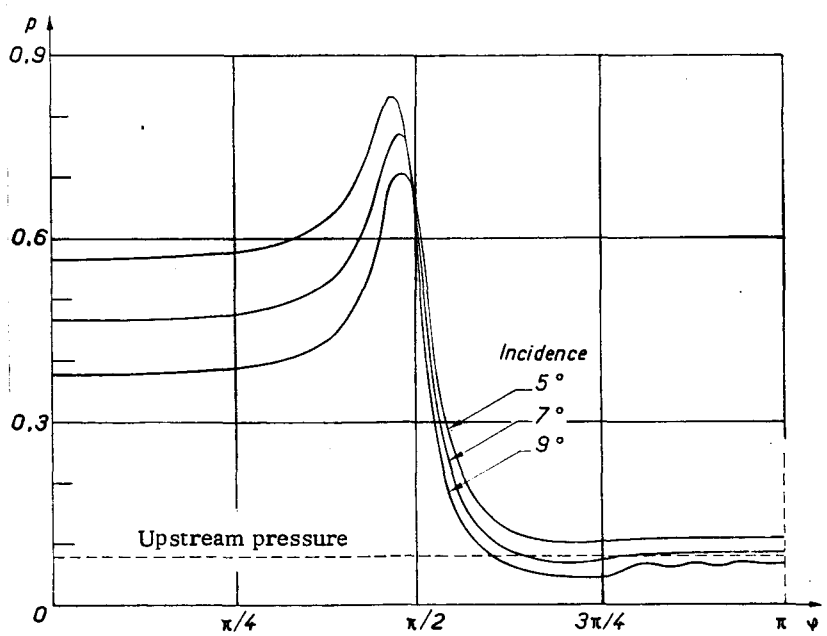

Figure 9. Pressure on Elliptical Cone (E) at Incidence.

($\mu = 20°$, $\lambda = 1/3$, $M_\infty = 7$)

1. Pressure on the Obstacle.

The pressure on the body varies little on the windward side, presents a very pronounced maximum corresponding to the regions of high curvature when φ is slightly less than $\pi/2$, then decreases rapidly to values close to the upstream pressure.

For incidences greater than 5°, the minimum is located outside the axis of symmetry on the leeward side; when the incidence increases, this minimum is pronounced and is surrounded by a zone in depression relative to the upstream flow, as in the case of a circular cone.

/17

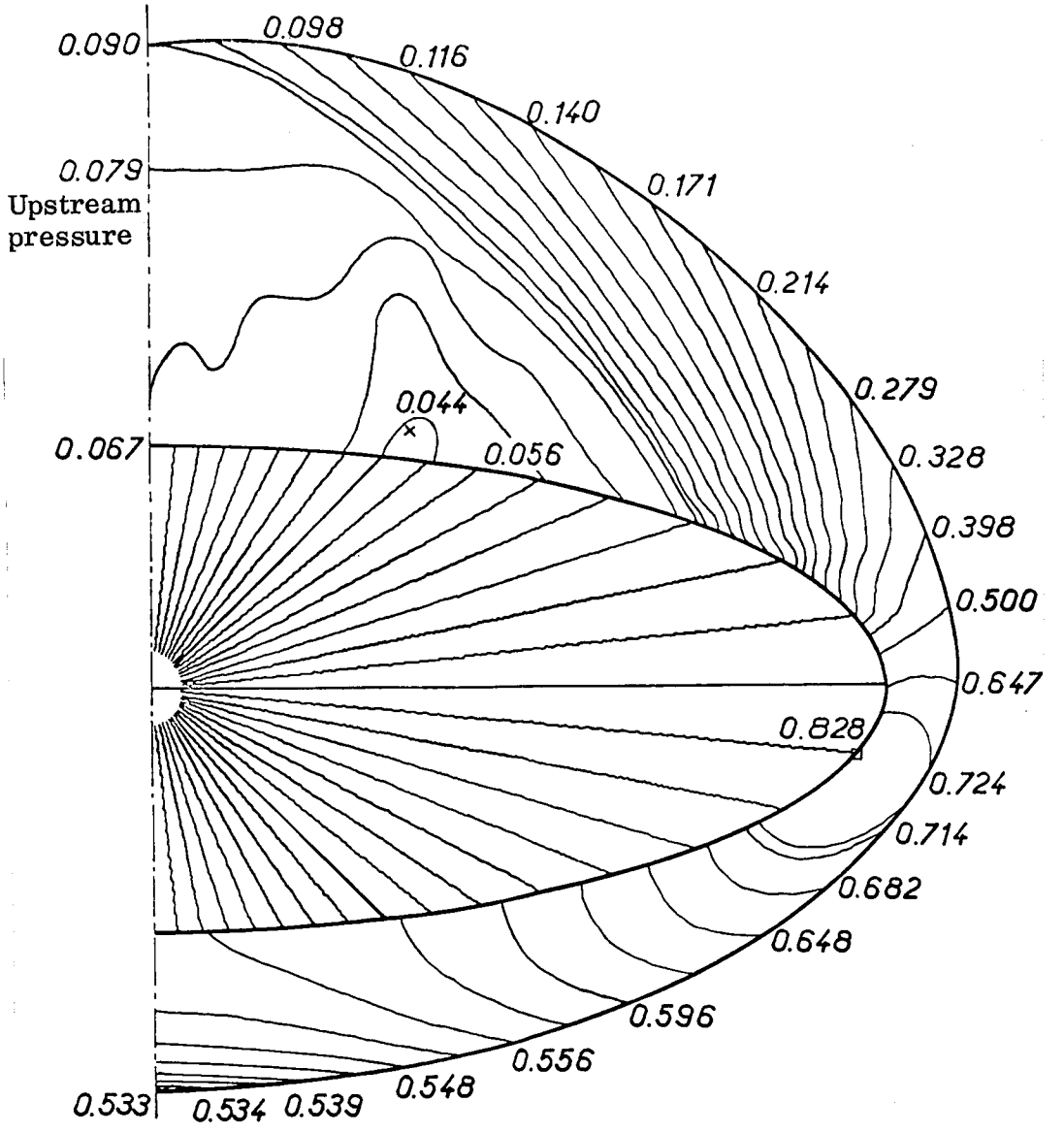

Figure 10. Curves p = Constant Around (E) at 9° Incidence.

(μ = 20°, λ = 1/3, M_∞ = 7)

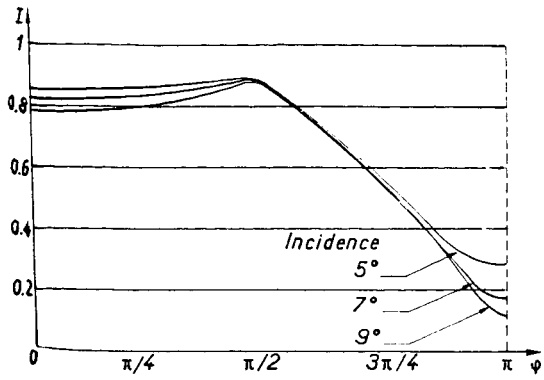

Figure 11. Intensity of the Shock for Different Incidences.

($\mu = 20°$, $\lambda = 1/3$, $M_\infty = 7$)

At 90° incidence, the pressure on the obstacle presents low-amplitude oscillations on the leeward side; the region where this phenomenon appears is a zone of marked depression (this may be due to an inaccuracy in the numerical results), and the shape of the isopiestic curves is much less regular in this region.

The pressure maximum is located on the obstacle for φ close to 80°, and the minimum is then in the interior of the slope near the body for $\varphi \simeq 135°$. The ratio of the extrema is of the order of 20, and the region of the obstacle with a high curvature on the leeward side presents very high pressure gradients, as shown in Fig. 10 by the density of the network of curves in this zone.

2. Intensity of the Shock.

Practically constant on the windward side, I passes through a maximum at φ close to 80°, then decreases linearly until it approaches the axis of symmetry on the leeward side.

A polynomial extrapolation from values of I and the axis of symmetry determines at about 13° the incidence i_c for which the shock degenerates into a Mach wave for $\varphi = \pi$.

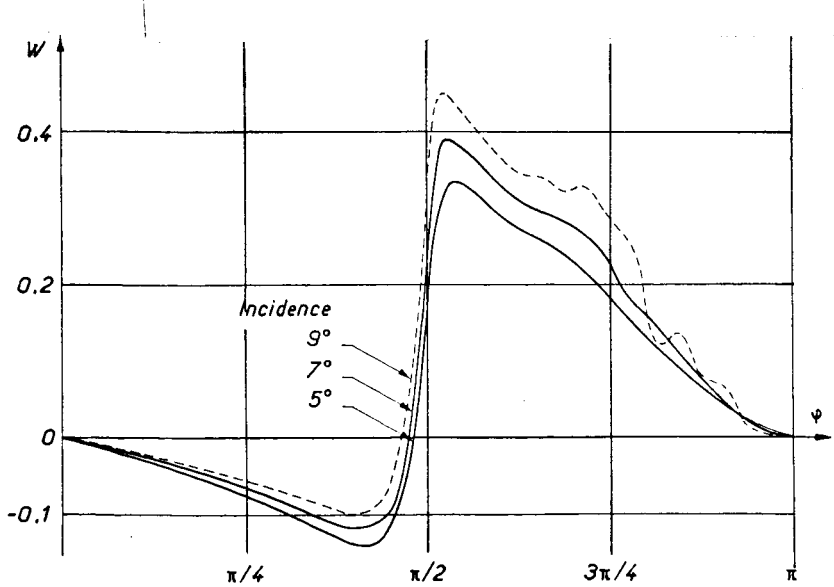

Figure 12. Component w on the Elliptical Cone (E).

($\mu = 20°$, $b/a = 1/3$, $M_\infty = 7$)

3. Field of Velocities.

The circumferential component of the velocity on the obstacle presents the minimum on the windward side; this component becomes zero before $\varphi = \pi/2$ (this point corresponds to a saddle point of the network of isentropic curves) and passes through the maximum on the leeward side before becoming zero again at $\varphi = \pi$. The curve w (φ) has very pronounced oscillations on the leeward side for 9° incidence (dotted line in Fig. 12). /18

Generally, the variations of w are very appreciable when the incidence increases; the convergence toward the conical solution is slower for this aerodynamic quantity.

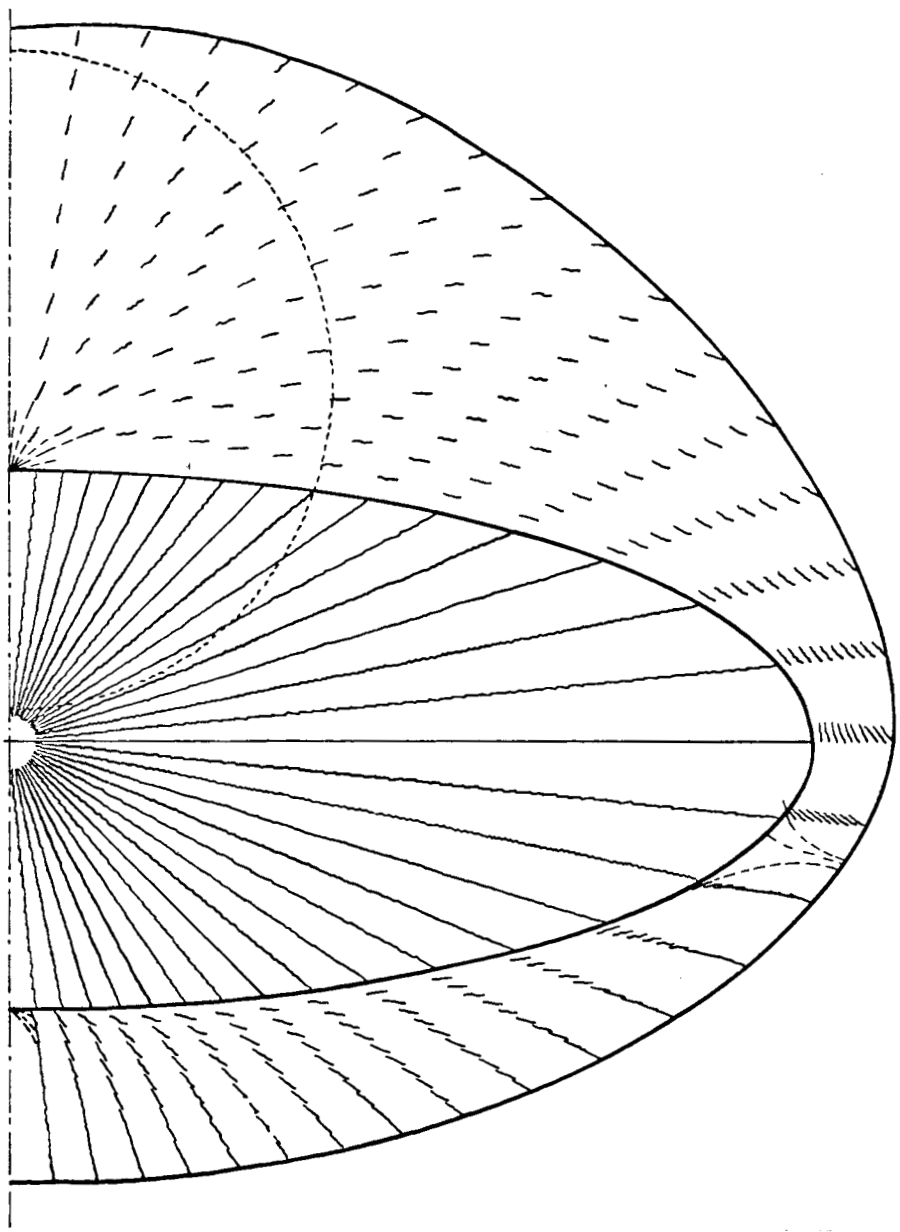

Figure 13. Fields of Entropic Direction.
($i = 9°$), ($\mu = 20°$, $b/a = 1/3$, $M_\infty = 7$)

The network of isentropic curves presents a saddle point on the obstacle at the point where w becomes zero, and there are two nodes on the axis of symmetry. These singularities are seen in Fig. 13.

For 11° incidence, we observe the same instability phenomenon as in the case of the circular cone, probably due to a singularity of the entropy located leeward outside the axis of symmetry.

4. Remarks

Since the convergence of the BVLR method is related to the slope of the characteristics (chapter IV of the first part of [1]), the flow becomes established much more rapidly on the windward side, where the shock is more violent; the values of the aerodynamic variables are much more regular there, and even in the cases of instability encountered, we assume that the precision of the calculations for $\varphi \in [0, \pi/2]$ is excellent.

Conclusion

/19

The BVLR method makes it possible to calculate the flow around conical obstacles at appreciable incidences; it appears that the shock wave remains closed even at incidences such that a part of the obstacle on the leeward side seems to be "protected" from the wind.

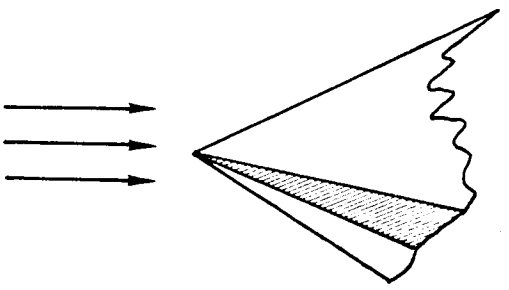

This brings out the fundamental differences between the cone and the dihedral at incidence, due to the respectively tridimensional and bidimensional character of the flows.

At high incidences, a depression zone exists downstream in the interior of the flow around the cone (at 9° incidence this region is quite sizable in the flow around (E), as shown by Figure 10).

When the incidence has reached a certain value i_c (approximately 12 and 13° respectively for the cones C and E), the depression zone extends up to the upstream flow, from which it is separated by a Mach wave (or a shock of zero intensity).

We have adopted a grid with a constant pitch in φ and used the linear function between the shock and the obstacle (in order to facilitate the programming in certain obvious ways).

It should be possible to construct a grid with a variable pitch in order to extend the scope of application of the method:

a) by multiplying the number of radii in the high-curvature regions of the obstacle in order to study the flow around cones approaching the delta wing in shape;

b) by choosing a nonlinear function ξ between the shock and the obstacle in order to try to estimate the numerical instabilities which arise at high incidences.

However, it is not certain that the solution is established satisfactorily on the leeward side at incidences greater than i_c (where the shock becomes evanescent) since the slope of the characteristics becomes low in the depression zone, and we then observe that the disturbances are damped very slowly in this region.

On the other hand, it is very probable that the finite difference scheme represents the flow imperfectly in the vicinity of the singularities of entropy; a satisfactory local treatment of the singular points is predicated on a complete mathematical analysis of the phenomena involved.

Let us specify some technical points about the program used: for a grid (ξ, φ) of a maximum of 700 points, the storage requirement for the data processor is less than 40,000 memory locations (the size of the grid could be slightly reduced when needed). The establishment of a flow around the conical body, virtually independent of the precision of the starting data (chosen to be compatible) takes up approximately 1 hour of control data CDC 3600 with a (10. 32) grid. The program is entirely written in Fortran language.

Manuscript submitted on July 10, 1967.

References

1. K.I. Babenko, G.P. Voskresenskiy, A.N. Lyubimov, and V.V. Rusanov. Three-Dimensional Flow of a Perfect Gas Around a Regular Body. "Nauka" Publishers, Moscow, 1964.
2. A. Ferri. Supersonic Flow Around Circular Cones at Angle of Attack. NACA, Rept. 1045 (1951).
3. R.E. Melnik. Vortical Singularities in Conical Flow. AIAA Journal, Vol. 5, (April 1967), pp. 631-637.

Translated for the National Aeronautics and Space Administration under Contract NASw-1694 by Scripta Technica, Inc.